

---

# Iterative Importance Fine-tuning of Diffusion Models

---

**Alexander Denker**

University College London  
a.denker@ucl.ac.uk

**Shreyas Padhy**

University of Cambridge  
sp2058@cam.ac.uk

**Francisco A. Vargas Palomo**

University of Cambridge  
fav25@cam.ac.uk

**Johannes Hertrich**

Université Paris Dauphine-PSL  
johannes.hertrich@dauphine.psl.eu

## Abstract

Diffusion models are an important tool for generative modelling, serving as effective priors in applications such as imaging and protein design. A key challenge in applying diffusion models for downstream tasks is efficiently sampling from resulting posterior distributions, which can be addressed using the  $h$ -transform. This work introduces a self-supervised algorithm for fine-tuning diffusion models by estimating the  $h$ -transform, enabling amortised conditional sampling. Our method iteratively refines the  $h$ -transform using a synthetic dataset resampled with path-based importance weights. We demonstrate the effectiveness of this framework on class-conditional sampling, inverse problems and reward fine-tuning for text-to-image diffusion models.

## 1 Introduction

Diffusion models have emerged as a powerful tool for generative modelling (Ho et al., 2020; Dhariwal and Nichol, 2021). As training these models is expensive and requires large amount of data, fine-tuning existing models for new tasks is of interest. In particular, given large pre-trained foundation models such as Stable Diffusion (Rombach et al., 2022) for images or RFDiffusion (Watson et al., 2023) for protein generation, the goal is to use the model as a prior for various downstream applications. For example, in imaging applications, the same diffusion model might be used as a prior for inpainting, deblurring or super-resolution tasks (Rout et al., 2024).

Sampling from the resulting conditional distribution can be interpreted as sampling from a tilted distribution (Domingo-Enrich et al., 2025), where the distribution defined by the pre-trained diffusion models  $p_{\text{data}}(\mathbf{x})$  is tilted by some reward or likelihood function  $r : \mathbb{R}^n \rightarrow \mathbb{R}$ . Then, we define the tilted distribution as

$$p_{\text{tilted}}(\mathbf{x}) \propto p_{\text{data}}(\mathbf{x}) \exp\left(\frac{r(\mathbf{x})}{\lambda}\right), \quad (1)$$

with a temperature  $\lambda > 0$ . This general framework includes several applications, such as statistical inverse problems with  $r(\mathbf{x}) = \ln p(\mathbf{y}|\mathbf{x})$  as the log-likelihood given observed measurements  $\mathbf{y}$ ; class conditional sampling with  $r(\mathbf{x}) = \ln p(c|\mathbf{x})$  as the log-class probabilities for a class  $c$  or reward fine-tuning where  $r(\mathbf{x})$  is learned explicitly as an image reward (Xu et al., 2024). The tilted distribution can also be expressed as the minimiser of an optimisation problem, i.e.,

$$p_{\text{tilted}} = \arg \min_p \{-\mathbb{E}_{\mathbf{x} \sim p}[r(\mathbf{x})] + \lambda \text{KL}(p, p_{\text{data}})\}. \quad (2)$$

Here, the first term maximises the reward, and the second term acts as a regulariser with the temperature  $\lambda$  as the regularisation strength. In the following, we directly incorporate  $\lambda$  into the reward  $r$  for an easier notation.

We can sample from the tilted distribution by adding an additional term, the generalised  $h$ -transform, to the drift function of the reverse SDE (Vargas et al., 2023b). The  $h$ -transform is in general intractable in closed form and thus many works propose approximations, see for example (Jalal et al., 2021; Chung et al., 2023; Rout et al., 2024). As an alternative, Denker et al. (2024) propose a supervised framework to estimate the  $h$ -transform given a small dataset from the tilted distribution. However, this limits the method to domains where such a dataset is available.

## 1.1 Contributions

In order to sample from the tilted distribution, we propose a self-supervised framework for estimating the  $h$ -transform without access to samples from the tilted distribution. Starting with an initial estimate of  $h$ , our method consists out of the following three steps.

1. First, we *sample a batch of trajectories from the diffusion model* with our current estimate of the  $h$ -transform.
2. Next, we use path-based importance weights to *filter the dataset* by rejecting samples which do not fit to the tilted distribution. Consequently, the filtered dataset describes the filtered distribution better than the original one. The corresponding importance weights can be computed on the fly during the first step and do not cause additional costs.
3. Finally, we use the supervised fine-tuning loss from Denker et al. (2024) to *update our estimation of the  $h$ -transform*.

From a theoretical viewpoint, we prove in Theorem 5 that our iterative importance fine-tuning decreases a certain loss function in each iteration, where the global minimiser of this loss function is known to coincide with the  $h$ -transform. Finally, we apply our method for class conditional sampling on MNIST, super-resolution, and reward-based fine-tuning of stable diffusion. We emphasize that our importance-based fine-tuning *does not require to differentiate the score function of the base-model and never considers more than one step of the generation process at once*. In particular, it can be applied for very large base-models where other methods run out of memory.

## 1.2 Related Work

**Controlled Generation from Diffusion Models** Controlled generation for diffusion models can be achieved via inference-time or post-training methods, see the recent review by Uehara et al. (2025). Inference-time methods, such as classifier guidance (Dhariwal and Nichol, 2021) or reconstruction guidance (Chung et al., 2023), guide the reverse diffusion process without additional training but typically increase computational cost and are often sensitive to hyperparameters (Song et al., 2024). Post-training techniques instead fine-tune models for a specific application. Fine-tuning comes with a higher initial computational cost but often results in reduced sampling time compared to inference-time methods (Denker et al., 2024). Supervised post-training methods require an additional task-specific dataset for fine-tuning (Ruiz et al., 2023; Zhang et al., 2023; Xu et al., 2024). In contrast, online post-training methods directly optimise some objective given by the reward function via reinforcement learning (Venkatraman et al., 2024; Clark et al., 2024; Fan et al., 2024; Black et al., 2024) or stochastic optimal control (Denker et al., 2024; Domingo-Enrich et al., 2025; Pidstrigach et al., 2025). Denoising diffusion samplers for via optimal control losses were considered by Albergo et al. (2023); Albergo and Vanden-Eijnden (2024); Berner et al. (2024); Blessing et al. (2025); Vargas et al. (2023a); Zhang and Chen (2022).

**Iterative retraining can cause model degradation** Iterative retraining of generative models on synthetic data has been shown to lead to performance degradation, including phenomena such as mode collapse (Alemohammad et al., 2024; Shumailov et al., 2023). Strategies to mitigate this issue have been proposed, such as mixing synthetic data with real data (Bertrand et al., 2024). Alternatively, training on curated synthetic datasets, i.e., choosing the synthetic data based on the reward  $r$ , has also been demonstrated to improve retraining stability and model performance (Dong et al., 2023; Ferbach et al., 2024). As we re-sample the synthetic dataset based on the importance

weights, our approach also falls into the category of retraining using curated data. However, as opposed to [Ferbach et al. \(2024\)](#) our selection process incorporates both the reward and the path probability, which can mitigate risks associated with iterative retraining.

**Self-supervised training for sampling** Recently, a number of self-supervised frameworks have been proposed for sampling from unnormalised densities, for example FAB ([Midgley et al., 2023](#)) or iDEM ([Akhound-Sadegh et al., 2024](#)). In iDEM, the authors propose an iterative framework, to train a diffusion model with a stochastic regression loss based on data sampled from the current estimation of the diffusion model. An importance-based acceptance-rejection scheme for improving the quality of generative models for sampling was proposed by [Hertrich and Gruhlke \(2024\)](#).

### 1.3 Outline

The rest of the paper is structured as follows. In Section 2 we give the necessary background on diffusion models and supervised fine-tuning. The path-based importance weights and the resampling step are presented in Section 3. We present experiments on class conditional sampling for MNIST, super-resolution, and reward-based fine-tuning of Stable Diffusion ([Rombach et al., 2022](#)) in Section 4. Conclusions are drawn in Section 5.

## 2 Background

Let us first recap the score-based generative modelling framework of [Song et al. \(2021\)](#); we start with a forward SDE, which progressively transforms the target distribution  $p_{\text{data}}$

$$d\mathbf{X}_t = f_t(\mathbf{X}_t) dt + \sigma_t d\overline{\mathbf{W}}_t, \quad \mathbf{X}_0 \sim p_{\text{data}}, \quad (3)$$

with drift  $f_t$  and diffusion  $\sigma_t$ . As usual, we denote by  $p_t$  the density of the solution  $\mathbf{X}_t$  at time  $t$  and by  $\tilde{p}_{t_1|t_2}(\mathbf{x}_{t_1}|\mathbf{x}_{t_2})$  the conditional densities of  $\mathbf{X}_{t_1}$  given  $\mathbf{X}_{t_2}$ . Under some regularity assumptions, there exists by [Anderson \(1982\)](#) a corresponding reverse SDE, that allows sampling from  $\mathbb{P}_T$  (typically  $\mathcal{N}(0, \mathbf{I}_n)$ ) and denoising them to generate samples from  $p_{\text{data}}$ . The reverse SDE is given by

$$d\mathbf{X}_t = (f_t(\mathbf{X}_t) - \sigma_t^2 s_t(\mathbf{X}_t)) dt + \sigma_t d\overline{\mathbf{W}}_t, \quad \mathbf{X}_T \sim \mathbb{P}_T, \quad (4)$$

where the time flows backwards and  $s_t(\mathbf{x}) = \nabla_{\mathbf{x}} \ln p_t(\mathbf{x})$  is the score function.

To sample from the tilted distribution  $p_{\text{tilted}}$  instead of  $p_{\text{data}}$ , we consider an additional guidance term in the reverse SDE. More precisely, we consider the SDE

$$d\mathbf{H}_t = (f_t(\mathbf{H}_t) - \sigma_t^2 (s_t(\mathbf{H}_t) + h_t(\mathbf{H}_t))) dt + \sigma_t d\overline{\mathbf{W}}_t, \quad (5)$$

where the time flows again backwards and we use  $\mathbf{H}_t$  for the guided reverse SDE. To ensure that  $\mathbf{H}_0 \sim p_{\text{tilted}}$ , [Denker et al. \(2024\)](#); [Vargas et al. \(2023b\)](#) considered a generalisation of Doob’s  $h$ -transform. Note that [Zhao et al. \(2025\)](#) prove a similar results to Theorem 1 (iii) from a reinforcement learning perspective.

**Theorem 1** (Proposition 2.2 and Theorem 3.1 in [Denker et al., 2024](#)).

Assume  $Z_r := \int \exp(r(\mathbf{x}_0)) d\mathbf{x}_0 < \infty$ . Further, let  $Q_T^{f_t}[p_{\text{tilted}}] := \int \tilde{p}_{T|0}(\mathbf{x}|\mathbf{x}_0) p_{\text{tilted}}(\mathbf{x}_0) d\mathbf{x}_0$  and

$$h_t^*(\mathbf{x}) = \nabla_{\mathbf{x}} \ln p_t^r(\mathbf{x}), \quad \text{where} \quad p_t^r(\mathbf{x}) = \int \frac{\exp(r(\mathbf{x}_0))}{Z_r} \tilde{p}_{0|t}(\mathbf{x}_0|\mathbf{x}) d\mathbf{x}_0. \quad (6)$$

Then, the following holds true:

- (i) Let  $(\mathbf{H}_t)_t$  be the solution of the SDE (5) with  $h_t = h_t^*$  given in (6) and  $\mathbf{H}_T \sim Q_T^{f_t}[p_{\text{tilted}}]$ . Then, it holds  $\mathbf{H}_0 \sim p_{\text{tilted}}$ .
- (ii) It holds that  $h_t^*$  is the unique minimiser of the score-matching (SM) loss function

$$\mathcal{L}_{SM}(h_t) = \mathbb{E}_{\substack{\mathbf{x}_0 \sim p_{\text{tilted}} \\ t \sim \mathcal{U}(0, T), \mathbf{x}_t \sim \tilde{p}_{t|0}(\cdot|\mathbf{x}_0)}} \left[ \left\| (h_t(\mathbf{x}_t) + s_t(\mathbf{x}_t)) - \nabla_{\mathbf{x}_t} \ln \tilde{p}_{t|0}(\mathbf{x}_t|\mathbf{x}_0) \right\|^2 \right]. \quad (7)$$

(iii) It holds that

$$h_t^* \in \arg \min_{h_t} \mathcal{F}(\mathbb{P}_h), \quad \text{where} \quad \mathcal{F}(\mathbb{P}) = \text{KL}(\mathbb{P}, \mathbb{P}_{\text{data}}) - \mathbb{E}_{\mathbf{x}_{[0,T]} \sim \mathbb{P}}[r(\mathbf{x}_0)] \quad (8)$$

and where  $\mathbb{P}_h$  and  $\mathbb{P}_{\text{data}}$  are the path measures of the corresponding SDEs (5) and (4).

**Remark 2.** In Theorem 1 (i) the terminal distribution is given as  $Q_T^{f_t}[p_{\text{tilted}}]$  instead of  $\mathbb{P}_T$  in Equation (4) to remove the value function bias. In Domingo-Enrich et al. (2025), the authors deal with the value function bias by altering the noise of the controlled SDE. However, due to the mixing time in the commonly used VP-SDE the discrepancy, measured w.r.t. the total variation distance, decays exponentially (Denker et al., 2024, Proposition G.2) and we approximate  $Q_T^{f_t}[p_{\text{tilted}}] \approx \mathbb{P}_T \approx \mathcal{N}(0, \mathbf{I}_n)$  for all numerical experiments.

Part (i) of Theorem 1 states conditions on  $h_t$  such that  $\mathbf{H}_0 \sim p_{\text{tilted}}$  in (5) and the (ii), (iii) provide loss functions to learn such a  $h_t$ . For the commonly used VP-SDE (Song et al., 2021), the loss (7) in part (ii) reduces to

$$\mathcal{L}_{SM}(h_t) = \mathbb{E}_{\substack{\mathbf{x}_0 \sim p_{\text{tilted}} \\ t \sim \text{U}(0,T), \mathbf{z} \sim \mathcal{N}(0,I)}} \left[ \|(h_t(\gamma_t \mathbf{x}_0 + \nu_t \mathbf{z}) + s_t(\gamma_t \mathbf{x}_0 + \nu_t \mathbf{z})) - \mathbf{z}/\nu_t\|^2 \right], \quad (9)$$

where the parameters  $\gamma_t, \nu_t$  are specified by the drift and diffusion coefficients. However, samples from the tilted distribution are often not available, making this approach limited in practice. Moreover, the loss function in (8) can be reformulated as a stochastic control (SC) loss, i.e.,

$$\mathcal{L}_{SC}(h_t) = \mathbb{E}_{\mathbf{x}_{[0,T]} \sim \mathbb{P}_h} \left[ \frac{1}{2} \int_0^T \sigma_t^2 \|h_t(\mathbf{x}_t)\|^2 dt - r(\mathbf{x}_0) \right]. \quad (10)$$

Differentiating  $\mathcal{L}_{SC}$  requires differentiating through the sample generation of the SDE. Even though Denker et al. (2024) reduce the computational cost of this step by using the VarGrad (Richter et al., 2020) or trajectory balance loss (Malkin et al., 2022), the memory requirements for optimising  $\mathcal{L}_{SC}$  still scale linearly with the number of steps in the SDE generation. Similar objectives have been considered from a reinforcement learning perspective, see e.g. Fan et al. (2024) using policy gradient methods (Schulman et al., 2017).

**Remark 3.** The connection of training diffusion models to stochastic optimal control have also been successfully exploited for sampling from unnormalised probability density function, see (Zhang and Chen, 2022; Nüsken and Richter, 2021; Berner et al., 2024). Further, the proof for Theorem 1 (iii) relies on connections to Schrödinger half-bridges (Heng et al., 2021; Vargas et al., 2021).

### 3 Self-Supervised Importance Fine-tuning

To circumvent the limitations of the supervised loss function considered by Denker et al. (2024), we propose in this section a self-supervised method for fine-tuning diffusion models. To this end, we combine the recently proposed rejection sampling steps from Hertrich and Gruhlke (2024) with the supervised fine-tuning from Theorem 1 (ii) and prove that this defines a descent algorithm for the loss function  $\mathcal{F}$  from Theorem 1 (iii).

#### 3.1 Importance-based Rejection

A basic tool for reweighting and fine-tuning generative models are importance weights. To this end, let  $\mathbf{x}_0$  be generated from the backward SDE (5) for some guidance term  $h$ . We assign to it the weight  $\frac{p_{\text{tilted}}(\mathbf{x}_0)}{p_h(\mathbf{x}_0)}$ , where  $p_h$  is the density of the generated distribution. Then, samples with a large importance weights are under-represented and samples with small importance weights are over-represented in  $p_h$  for approximating  $p_{\text{tilted}}$ .

Unfortunately, we do not have access to the explicit value of  $p_h$ . Therefore, we rewrite the importance weight with  $p_{\text{tilted}}(\mathbf{x}) \propto p_{\text{data}}(\mathbf{x}) \exp(r(\mathbf{x}))$  as

$$\frac{p_{\text{tilted}}(\mathbf{x})}{p_h(\mathbf{x})} = \frac{p_{\text{tilted}}(\mathbf{x})}{p_{\text{data}}(\mathbf{x})} \frac{p_{\text{data}}(\mathbf{x})}{p_h(\mathbf{x})} \propto \exp(r(\mathbf{x})) \frac{p_{\text{data}}(\mathbf{x})}{p_h(\mathbf{x})}. \quad (11)$$



---

**Algorithm 1** Self-supervised estimation of the  $h$ -transform for DDPM

---

**Require:** Pre-trained noise prediction model  $\epsilon_t^\theta(\mathbf{x}_t)$ , noise schedule  $\bar{\alpha}_t$

**Require:** Number of outer training steps  $K$ , number of inner training steps  $M$ , number of samples  $N$ , batch size  $m$ , buffer with maximum length

**Require:** Rate of accepted samples  $r$

```

1: for  $k = 1$  to  $K$  do
2:   Sample  $\mathbf{x}_{[0:T]}^{(1:N)} \sim \mathbb{P}_{h_\varphi}$  ▷ Sample paths with current model
3:   for  $i = 1$  to  $N$  do ▷ Resample using rejection sampling
4:     Compute acceptance probability  $\alpha(\mathbf{x}_{[0:T]}^{(i)})$ 
5:     Sample  $u \sim U([0, 1])$ 
6:     If  $u \leq \alpha(\mathbf{x}_{[0:T]}^{(i)})$ , add  $\mathbf{x}_{[0:T]}^{(i)}$  to buffer
7:   for  $1$  to  $M$  do ▷ Inner training loop using buffer
8:     Sample  $\mathbf{x}^{(1:m)}$  from buffer
9:      $t \sim U(\{1, \dots, T\})$ 
10:     $\epsilon \sim \mathcal{N}(0, I)$ 
11:     $\mathbf{x}_t^{(1:m)} \leftarrow \sqrt{\bar{\alpha}_t} \mathbf{x}^{(1:m)} + \sqrt{1 - \bar{\alpha}_t} \epsilon$ 
12:     $\ell \leftarrow \left\| \left( \epsilon_t^\theta(\mathbf{x}_t^{(1:m)}) + h_t^\varphi(\mathbf{x}_t^{(1:m)}) \right) - \epsilon \right\|_2^2$ 
13:     $\varphi \leftarrow \text{Optim}(\varphi, \nabla_\varphi \ell)$ 

```

---

Now we approximate the quotient  $\frac{p_{\text{data}}(\mathbf{x})}{p_h(\mathbf{x})}$  by the RND, such that

$$\frac{p_{\text{tilted}}(\mathbf{x})}{p_h(\mathbf{x})} \propto \exp(r(\mathbf{x})) \frac{p_{\text{data}}(\mathbf{x})}{p_h(\mathbf{x})} \approx \exp(r(\mathbf{x}_0)) \frac{d\mathbb{P}_{\text{data}}}{d\mathbb{P}_h}(\mathbf{x}_{[0,T]}) \quad (12)$$

where  $\mathbb{P}_h$  and  $\mathbb{P}_{\text{data}}$  are the path measures for the SDEs corresponding to the prior and adjusted diffusion model and  $\mathbf{x}_{[0:T]} = (\mathbf{x}_t)_{t \in [0,T]}$  is the whole generated trajectory. The Radon-Nikodym derivative  $\frac{d\mathbb{P}_{\text{data}}}{d\mathbb{P}_h}(\mathbf{x}_{[0,T]})$  can now be computed based on the framework from [Vargas et al. \(2024\)](#). We summarise the result in the following lemma. The derivations are included in Appendix A, both in continuous and in discrete time.

**Lemma 4.** *The right side of (12) can be rewritten as*

$$\exp \left( r(\mathbf{x}_0) - \frac{1}{2} \int_0^T \sigma_t^2 \|h_t(\mathbf{x}_t)\|_2^2 dt + \int_0^T \sigma_t h_t(\mathbf{x}_t)^\top dW_t \right), \quad (13)$$

for  $\mathbf{x}_{[0:T]} \sim \mathbb{P}_h$ .

These path-wise importance weights can be computed concurrently with sampling without any computational overhead. For numerical stability, we perform these computations in the log-space.

In practice, importance weights have the disadvantage that they often suffer from highly imbalanced weights. As a remedy, [Hertrich and Gruhlke \(2024\)](#) proposed a rejection sampling algorithm based on relaxed importance weights. Plugging in our approximation (12), this rejection sampling step amounts to computing, for some generated trajectory  $\mathbf{x}_{[0,T]}$ , the acceptance probability

$$\alpha(\mathbf{x}_{[0,T]}) = \min \left( 1, \frac{d\mathbb{P}_{\text{data}}}{d\mathbb{P}_h}(\mathbf{x}_{[0,T]}) \frac{\exp(r(\mathbf{x}_0))}{c} \right), \quad (14)$$

where  $c$  is a hyper-parameter. In practice, we use an adaptive choice of  $c$  such that a certain rate of samples is accepted, see ([Hertrich and Gruhlke, 2024](#), Rem 10). We will show in the next subsection that the distribution of accepted samples is closer to the tilted distribution than the distribution of the initially generated samples.

### 3.2 Self-supervised Importance Fine-Tuning

Next, we will combine the importance-based rejection steps with the supervised loss function from Theorem 1 (ii) to obtain a tractable fine-tuning algorithm. More precisely, starting with an initial

guidance term  $h^0$  we construct a sequence of guidance terms  $h^k$  for  $k = 1, 2, \dots$  by the following steps.

First, we sample a batch  $\{\mathbf{x}_0^{(i)}\}_{i=1,\dots,N}$  from the reverse SDE (5) with  $h = h^k$  and compute the corresponding acceptance probabilities  $\alpha_i = \alpha(\mathbf{x}_{[0,T]}^{(i)})$  from (14). Second, we keep any sample from the batch with probability  $\alpha_i$  and discard the rest. We denote the distribution of remaining samples by  $\tilde{\mathbb{P}}_{h^k}^0$ . Finally, we update the guidance term  $h^k$  by using the supervised loss function for the  $h$ -transform from Theorem 1 (ii). That is, we define  $h^{k+1} \in \arg \min_g \mathcal{L}_{FT}(g)$ , where

$$\mathcal{L}_{FT}(g) = \mathbb{E}_{\substack{\mathbf{x}_0 \sim \tilde{\mathbb{P}}_{h^k}^0 \\ t \sim \mathcal{U}(0,T), \mathbf{x}_t \sim \tilde{\mathcal{P}}_{t|0}(\cdot|\mathbf{x}_0)}} \left[ \left\| (g_t(\mathbf{x}_t) + s_t(\mathbf{x}_t)) - \nabla_{\mathbf{x}_t} \ln \tilde{p}_{t|0}(\mathbf{x}_t|\mathbf{x}_0) \right\|^2 \right]. \quad (15)$$

We summarise our self-supervised importance fine-tuning in Algorithm 1 for the discrete DDPM framework (Ho et al., 2020).

Recall that the generalised  $h$ -transform from Theorem 1 minimises the function  $\mathcal{F}(\mathbb{P}_h) = \text{KL}(\mathbb{P}_h, \mathbb{P}_{\text{data}}) - \mathbb{E}_{\mathbf{x}_{[0,T]} \sim \mathbb{P}_h} [r(\mathbf{x}_0)]$ . The following theorem proves that our self-supervised importance fine-tuning is a descent algorithm for  $\mathcal{F}$ . More precisely, it holds that  $\mathcal{F}(\mathbb{P}_{h^{k+1}}) \leq \mathcal{F}(\mathbb{P}_{h^k})$  for all  $k = 1, 2, \dots$ . We include the proof in Appendix B.1.

**Theorem 5.** *Let  $\alpha(\mathbf{x}_{[0,T]}) = \min \left( 1, \frac{d\mathbb{P}_{\text{data}}}{d\mathbb{P}_h}(\mathbf{x}_{[0,T]}) \frac{\exp(r(\mathbf{x}_0))}{c} \right)$  be the acceptance probability of a sample  $\mathbf{x}_{[0,T]} \sim \mathbb{P}_h$  and denote by  $\tilde{\mathbb{P}}_h$  the distribution of the accepted paths. Then, the following holds true:*

- (i)  $\frac{d\tilde{\mathbb{P}}_h}{d\mathbb{P}_h}(\mathbf{x}_{[0,T]}) = \frac{\alpha(\mathbf{x}_{[0,T]})}{\mathbb{E}_{\mathbf{x}_{[0,T]} \sim \mathbb{P}_h} [\alpha(\mathbf{x}_{[0,T]})]}$
- (ii)  $\mathcal{F}(\tilde{\mathbb{P}}_h) \leq \mathcal{F}(\mathbb{P}_h)$ , where  $\mathcal{F}(\mathbb{P}) = \text{KL}(\mathbb{P}, \mathbb{P}_{\text{data}}) - \mathbb{E}_{\mathbf{x}_{[0,T]} \sim \mathbb{P}} [r(\mathbf{x}_0)] \propto \text{KL}(\mathbb{P}, \mathbb{P}_{\text{tilde}})$
- (iii) Let  $h_t^* \in \arg \min_{g_t} \mathcal{L}_{FT}(g_t)$  with  $\mathcal{L}_{FT}$  from (15) and let  $\mathbb{P}_{h^*}$  be the path measure of the corresponding SDE. Then it holds  $\mathcal{F}(\mathbb{P}_{h^*}) \leq \mathcal{F}(\tilde{\mathbb{P}}_h) \leq \mathcal{F}(\mathbb{P}_h)$ .

### 3.3 Training and Network Parametrisation

**Replay buffer** Sampling from the current model is the most computationally expensive part of the algorithm. Motivated by Midgley et al. (2023); Sendera et al. (2024), we make use of an unprioritised replay buffer with a fixed length. We save the accepted samples from the current model and append them the buffer. Once the fixed length is reached, we discard the oldest samples. During training, we randomly sample batches from the buffer.

**Network parametrisation** The parametrisation of the  $h$ -transform has a crucial effect on performance and convergence speed (He et al., 2025). Motivated by the network parametrisation in sampling applications with diffusion (Vargas et al., 2023a; Zhang and Chen, 2022) and fine-tuning approaches (Denker et al., 2024; Venkatraman et al., 2024), we make use of a *reward-informed inductive bias* given as

$$h_t^\theta(\mathbf{x}_t) = \text{NN}_1(\mathbf{x}_t, t) + \text{NN}_2(t) \nabla_{\hat{\mathbf{x}}_0} r(\hat{\mathbf{x}}_0), \quad (16)$$

where  $\hat{\mathbf{x}}_0$  is the Tweedie estimate given the pre-trained unconditional diffusion model,  $\text{NN}_1$  is a vector-valued and  $\text{NN}_2$  a scalar-valued neural network. We initialise the last layer of  $\text{NN}_1$  to be zero and  $\text{NN}_2$  to be constant. However, for text-to-image diffusion models we instead make use of prior work, see e.g. (Venkatraman et al., 2024; Fan et al., 2024), and use the parameter efficient LoRA method (Hu et al., 2022).

**KL-Regularisation** Similar to Fan et al. (2024), we found that using a KL regulariser was useful to improve diversity in the supervised setting. The KL divergence between  $p_h$  and  $p_{\text{data}}$  can be bounded as

$$D_{\text{KL}}(p_h, p_{\text{data}}) \leq D_{\text{KL}}(\mathbb{P}_h, \mathbb{P}_{\text{data}}) = \mathbb{E}_{\mathbf{H}_t \sim \mathbb{P}_h} \left[ \int_0^T \sigma_t^2 \|h_t(\mathbf{H}_t)\|_2^2 dt \right], \quad (17)$$

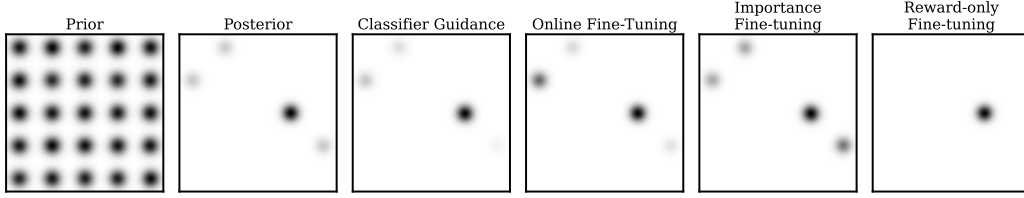


Figure 1: 2D Toy example for fine-tuning diffusion models. We show the prior the log-probability of the tilted distribution and samples from the conditional diffusion model using classifier guidance (Dhariwal and Nichol, 2021), online fine-tuning (Fan et al., 2024), our importance fine-tuning and a variation with only reward-based importance weights.

i.e., the norm of the  $h$ -transform over trajectories, see Appendix A for a derivation. The naive addition of this term to the supervised training loss is expensive, as one has to backpropagate through the full trajectory. Instead, we estimate the integral using a single random time step.

## 4 Experiments

In this section, we present a toy example on a 2D dataset, class conditional sampling for MNIST, super-resolution, and finally results for reward fine-tuning of text-to-image diffusion models. The code is available<sup>1</sup>

### 4.1 2D Toy example

As an initial example we make use of a diffusion trained on samples of a Gaussian mixture model (GMM) with 25 modes, arranged on a grid. The goal is to sample from the tilted distribution  $p_{\text{data}}(\mathbf{x}) \exp(r(\mathbf{x}))$ , where the reward  $r$  is defined as the log-likelihood of a GMM with a reweighted subset of the modes, see Appendix C.1 for the detailed setup. Figure 1 illustrates both the prior and the density of the tilted distribution. We compare against Classifier Guidance (Dhariwal and Nichol, 2021), an inference time method, where the  $h$ -transform is approximated by the gradient of the reward  $h_t(\mathbf{x}_t) = \gamma \nabla_{\mathbf{x}_t} r(\mathbf{x}_t)$ . Further, we compare against online fine-tuning, where we directly optimise Equation (2). Instead of employing the policy gradient of DPOK (Fan et al., 2024), we backpropagate gradients through the entire trajectory for this low-dimensional toy example. Further, we evaluate our importance fine-tuning and a variation where importance weights are calculated solely based on the reward, referred to as reward-only fine-tuning.

In Figure 1, we observe that classifier guidance is able to find all the modes of the posterior, fails to capture the correct weighting. In contrast, both online fine-tuning and importance fine-tuning yield samples that more accurately represent the target distribution. Lastly, the reward-only fine-tuning method collapses to the highest mode.

### 4.2 Posterior Sampling for Inverse Problems

We consider the task of posterior sampling in inverse problems. Here, the reward function  $r$  is given by the likelihood  $p^{\text{lkhd}}(\mathbf{y}|\mathbf{x})$ , i.e., the conditional distributions of measurements  $\mathbf{y}$  given images  $\mathbf{x}$ . We focus on the linear inverse problem of super-resolution, where the measurements are given as  $\mathbf{y}^\delta = \mathbf{A}\mathbf{x} + \eta$ . Here,  $\mathbf{A}$  is the downsampling operator,  $\eta \sim \mathcal{N}(0, \sigma_y^2 \mathbf{I})$  represents additive Gaussian noise, and the likelihood is given as  $r(\mathbf{x}; \mathbf{y}^\delta) = \ln p^{\text{lkhd}}(\mathbf{y}^\delta|\mathbf{x}) = -\frac{1}{2\sigma_y^2} \|\mathbf{A}\mathbf{x} - \mathbf{y}^\delta\|_2^2$ .

We train a diffusion model on the Flowers dataset (Nilsback and Zisserman, 2008) and consider the  $2\times$  super-resolution task with 5% relative Gaussian noise. For the  $h$ -transform we make use of the reward-informed architecture (16), see Appendix C.2 for the detailed setup. Theorem 5 demonstrates that iterative importance fine-tuning functions as a descent algorithm for the SC loss  $\mathcal{L}_{\text{SC}}$ . Figure 2 presents both the SC loss across iterations and the final model’s sample outputs, confirming that iterative fine-tuning operates as a descent algorithm for the SC loss in this scenario.

<sup>1</sup><https://anonymous.4open.science/r/IterativeImportanceFinetuning-4606>

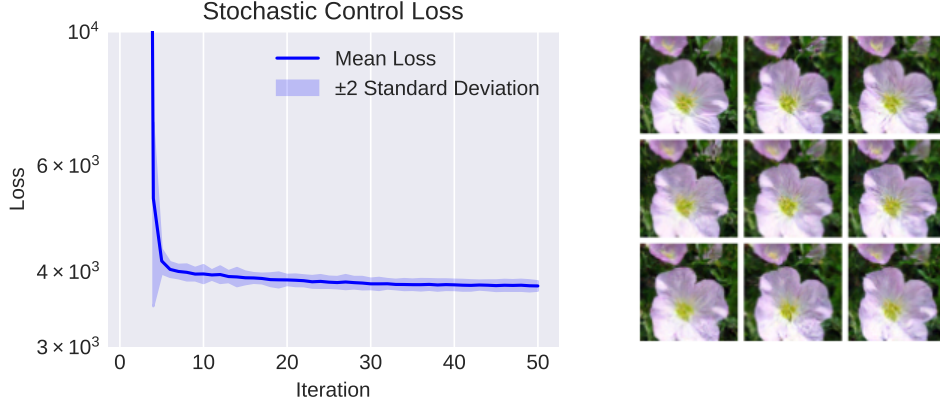


Figure 2: Posterior sampling for Flowers. Left: We show decay of the SC loss function  $\mathcal{L}_{SC}(h_k)$  over fine-tuning iterations  $k$ . We show the mean loss over 10 independent training runs with  $\pm 2$  std intervals. Right: The upper left image is the ground truth image and the remaining 8 images are samples from the model.

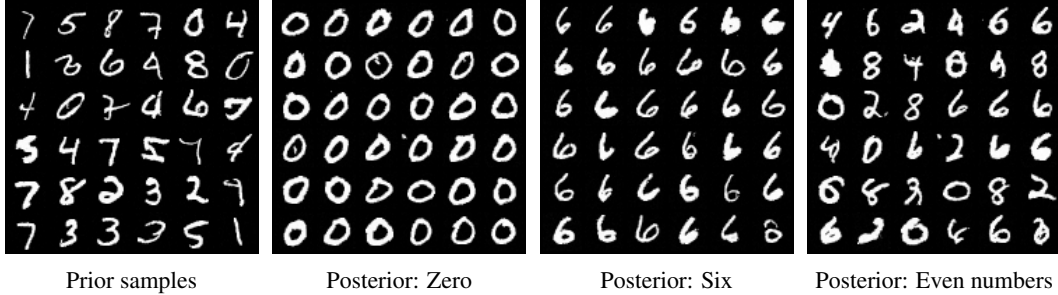


Figure 3: Class conditional sampling for MNIST. Left: Sampled from unconditional model. Middle: Samples for class ‘six’. Right: Samples for even numbers.

### 4.3 Class-conditional sampling

As another application, we consider class conditional sampling. Let  $c$  be the class and  $p(c|\mathbf{x})$  the log class probabilities of a pre-trained classifier. The goal is to sample from the tilted distribution with the reward as  $r(\mathbf{x}) = \ln p(c|\mathbf{x})$ . We consider both the MNIST dataset and pre-train unconditional diffusion models using the U-Net architecture from Ho et al. (2020). We use a convolutional classifier with a 98.6% accuracy. We use the reward-informed architecture as in Eqn. (16).

We use importance fine-tuning to learn the posterior for different MNIST classes and for even/odd numbers. We show posterior prior samples in Figure 3, see Figure 5 for all classes. We compare both against classifier guidance and online fine-tuning. For online fine-tuning we optimise Equation (10) using VarGrad (Richter et al., 2020) to reduce the memory cost. In Table 1 we present the expectation of the reward and the FID (Heusel et al., 2017) based on the features of the penultimate layer of the pre-trained classifier. For single-class posteriors, online fine-tuning achieves a higher expected reward. A similar trend is observed for even/odd tasks. This indicates that online fine-tuning is more effective at maximising reward for this setting, although at the expense of reduced sample diversity, as reflected by the FID score.

Table 1: Expected reward and FID scores for class conditional sampling on MNIST.

Method	Single class		Even / Odd	
	$\mathbb{E}[r(\mathbf{x})]$ ( $\uparrow$ )	FID ( $\downarrow$ )	$\mathbb{E}[r(\mathbf{x})]$ ( $\uparrow$ )	FID ( $\downarrow$ )
Classifier Guid.	-1.495	117.241	-2.572	193.984
Online FT	-0.110	31.994	-0.065	198.871
Importance FT	-0.152	30.814	-0.878	110.403



Figure 4: Samples for the base model, DPOK, Adjoint Matching and our importance FT for the prompt "A green colored rabbit.". Images were generated using the same seed.

Table 2: Results for text-to-image. We compute the mean reward and diversity over 100 samples.

	"A green colored rabbit."		"Two roses in a vase."		"Two dogs in the park."		GPU hrs (train)	Peak GPU memory
	Reward ( $\uparrow$ )	Diversity ( $\uparrow$ )	Reward ( $\uparrow$ )	Diversity ( $\uparrow$ )	Reward ( $\uparrow$ )	Diversity ( $\uparrow$ )		
Base Model	-0.207	0.154	1.130	0.108	0.518	0.193	N/A	9GB
Top-K Sampling	1.334	0.149	1.619	0.121	0.970	0.161	N/A	9GB
DPOK	1.621	0.065	1.592	0.106	1.013	0.144	28 (A100)	34 GB
Adjoint Matching	1.706	0.050	1.504	0.088	1.325	0.132	4 (A100)	36 GB
Importance FT (ours)	1.462	0.051	1.534	0.077	1.010	0.120	7 (RTX 4090)	16 GB

#### 4.4 Text-to-Image Reward Fine-tuning

Despite the progress in training text-to-image diffusion models, samples not always align with human preferences. In particular, the model can struggle with unnatural prompts such as "A green rabbit" (Venkatraman et al., 2024; Fan et al., 2024). To alleviate this problem, the diffusion model is fine-tuned to maximise some reward model, trained to imitate human preferences. We use the latent diffusion model Stable Diffusion-v1.5 (Rombach et al., 2022) and align it using the ImageReward-v1.0 (Xu et al., 2024) reward model. We refer to Appendix C.4 for experimental details. We compare against Top- $K$  sampling ( $K = 6$ ) as a training-free baseline, where  $K$  samples are generated, and the one with the highest reward is selected, increasing sampling time by a factor of  $K$ . Additionally, we evaluate against two state-of-the-art methods, i.e., DPOK (Fan et al., 2024) and adjoint matching (Domingo-Enrich et al., 2025). Both DPOK and our method use LoRA parametrization, whereas adjoint matching fine-tunes the full model. Consequently, DPOK runs on an RTX 4090 with 24GB memory (using a tiny batch size and checkpointing), while adjoint matching demands a GPU with over 30GB memory. Results are presented in Table 2 and images are shown in Figure 4, see Appendix C.4 for additional results. We present both the mean reward and the diversity, measured as one minus the mean cosine similarity of CLIP embeddings. While our method exhibits slightly lower performance in reward scores compared to adjoint matching, it enables fine-tuning using only a single smaller GPU. This makes our approach more accessible for researchers with limited computational resources, and it could be scaled further with hardware upgrades.

## 5 Conclusion

We propose an iterative approach for fine-tuning diffusion models for conditional sampling tasks. As the naive iterative retraining of generative models often lead to performance degradation (Shumailov et al., 2023), we introduce an additional resampling step based on path-based importance weights. We show initial evaluations for class conditional sampling and reward fine-tuning of text-to-image diffusion models. Online fine-tuning methods often require additional tricks to increase training stability, e.g., Venkatraman et al. (2024) use loss clipping and disregard low reward trajectories or Fan et al. (2024) employ variance reduction techniques by additionally learning the value function. In contrast our importance fine-tuning method is trained using a score matching loss, see Theorem 1, leading to a more stable training.

**Limitations** In our iterative refinement method, the model is fine-tuned using "good", i.e., having a high importance weight, samples from the pre-trained model. However, these samples necessarily lie in the support of the pre-trained model and we rely on the fact that such "good" samples exist. Thus, our refinement approach might struggle on domains where the distribution of the pre-trained model is sparse and high reward samples are rare. One possibility to alleviate this problem is to make use of "off-policy" samples (Venkatraman et al., 2024), which are obtained by some other method.



For off-policy samples, we loose the compact formulation of the RND from Lemma 4. However, we can still compute importance weights using the RND in Proposition 6, see Appendix A.

**Potential Societal Impacts** Diffusion models, as a class of generative models, have potential negative societal impacts. Fine-tuning diffusion models according to an external reward function, can for example potentially be used to generate deepfakes and spread disinformation.

## References

- Akhound-Sadegh, T., Rector-Brooks, J., Bose, J., Mittal, S., Lemos, P., Liu, C.-H., Sendera, M., Ravanbakhsh, S., Gidel, G., Bengio, Y., Malkin, N., and Tong, A. (2024). Iterated denoising energy matching for sampling from boltzmann densities. In *Forty-first International Conference on Machine Learning*.
- Albergo, M. S., Boffi, N. M., and Vanden-Eijnden, E. (2023). Stochastic interpolants: A unifying framework for flows and diffusions. *arXiv preprint arXiv:2303.08797*.
- Albergo, M. S. and Vanden-Eijnden, E. (2024). Nets: A non-equilibrium transport sampler. *arXiv preprint arXiv:2410.02711*.
- Alemohammad, S., Casco-Rodriguez, J., Luzi, L., Humayun, A. I., Babaei, H., LeJeune, D., Siahkoochi, A., and Baraniuk, R. (2024). Self-consuming generative models go MAD. In *The Twelfth International Conference on Learning Representations*.
- Anderson, B. D. (1982). Reverse-time diffusion equation models. *Stochastic Processes and their Applications*, 12(3):313–326.
- Berner, J., Richter, L., and Ullrich, K. (2024). An optimal control perspective on diffusion-based generative modeling. *Transactions on Machine Learning Research*.
- Bertrand, Q., Bose, J., Duplessis, A., Jiralerspong, M., and Gidel, G. (2024). On the stability of iterative retraining of generative models on their own data. In *The Twelfth International Conference on Learning Representations*.
- Black, K., Janner, M., Du, Y., Kostrikov, I., and Levine, S. (2024). Training diffusion models with reinforcement learning. In *The Twelfth International Conference on Learning Representations*.
- Blessing, D., Berner, J., Richter, L., and Neumann, G. (2025). Underdamped diffusion bridges with applications to sampling. In *The Thirteenth International Conference on Learning Representations*.
- Chung, H., Kim, J., Mccann, M. T., Klasky, M. L., and Ye, J. C. (2023). Diffusion posterior sampling for general noisy inverse problems. In *The Eleventh International Conference on Learning Representations*.
- Clark, K., Vicol, P., Swersky, K., and Fleet, D. J. (2024). Directly fine-tuning diffusion models on differentiable rewards. In *The Twelfth International Conference on Learning Representations*.
- Denker, A., Vargas, F., Padhy, S., Didi, K., Mathis, S. V., Barbano, R., Dutordoir, V., Mathieu, E., Komorowska, U. J., and Lio, P. (2024). DEFT: Efficient fine-tuning of diffusion models by learning the generalised  $\mathbb{H}$ -transform. In *The Thirty-eighth Annual Conference on Neural Information Processing Systems*.
- Dhariwal, P. and Nichol, A. (2021). Diffusion models beat gans on image synthesis. *Advances in neural information processing systems*, 34:8780–8794.
- Domingo-Enrich, C., Drozdal, M., Karrer, B., and Chen, R. T. Q. (2025). Adjoint matching: Fine-tuning flow and diffusion generative models with memoryless stochastic optimal control. In *The Thirteenth International Conference on Learning Representations*.
- Dong, H., Xiong, W., Goyal, D., Zhang, Y., Chow, W., Pan, R., Diao, S., Zhang, J., SHUM, K., and Zhang, T. (2023). RAFT: Reward ranked finetuning for generative foundation model alignment. *Transactions on Machine Learning Research*.



- Fan, Y., Watkins, O., Du, Y., Liu, H., Ryu, M., Boutilier, C., Abbeel, P., Ghavamzadeh, M., Lee, K., and Lee, K. (2024). Reinforcement learning for fine-tuning text-to-image diffusion models. *Advances in Neural Information Processing Systems*, 36.
- Ferbach, D., Bertrand, Q., Bose, J., and Gidel, G. (2024). Self-consuming generative models with curated data provably optimize human preferences. In *The Thirty-eighth Annual Conference on Neural Information Processing Systems*.
- He, J., Du, Y., Vargas, F., Zhang, D., Padhy, S., OuYang, R., Gomes, C., and Hernández-Lobato, J. M. (2025). No trick, no treat: Pursuits and challenges towards simulation-free training of neural samplers. *arXiv preprint arXiv:2502.06685*.
- Heng, J., De Bortoli, V., Doucet, A., and Thornton, J. (2021). Simulating diffusion bridges with score matching. *arXiv preprint arXiv:2111.07243*.
- Hertrich, J. and Gruhlke, R. (2024). Importance corrected neural JKO sampling. *arXiv preprint arXiv:2407.20444*.
- Heusel, M., Ramsauer, H., Unterthiner, T., Nessler, B., and Hochreiter, S. (2017). Gans trained by a two time-scale update rule converge to a local nash equilibrium. *Advances in neural information processing systems*, 30.
- Ho, J., Jain, A., and Abbeel, P. (2020). Denoising diffusion probabilistic models. *Advances in neural information processing systems*, 33:6840–6851.
- Ho, J. and Salimans, T. (2022). Classifier-free diffusion guidance. *arXiv preprint arXiv:2207.12598*.
- Hu, E. J., yelong shen, Wallis, P., Allen-Zhu, Z., Li, Y., Wang, S., Wang, L., and Chen, W. (2022). LoRA: Low-rank adaptation of large language models. In *International Conference on Learning Representations*.
- Jalal, A., Arvinte, M., Daras, G., Price, E., Dimakis, A. G., and Tamir, J. (2021). Robust compressed sensing mri with deep generative priors. *Advances in Neural Information Processing Systems*, 34:14938–14954.
- Léonard, C. (2014). Some properties of path measures. *Séminaire de Probabilités XLVI*, pages 207–230.
- Loshchilov, I. and Hutter, F. (2019). Decoupled weight decay regularization. In *International Conference on Learning Representations*.
- Malkin, N., Jain, M., Bengio, E., Sun, C., and Bengio, Y. (2022). Trajectory balance: Improved credit assignment in gflownets. *Advances in Neural Information Processing Systems*, 35:5955–5967.
- Midgley, L. I., Stimper, V., Simm, G. N. C., Schölkopf, B., and Hernández-Lobato, J. M. (2023). Flow annealed importance sampling bootstrap. In *The Eleventh International Conference on Learning Representations*.
- Nilsback, M.-E. and Zisserman, A. (2008). Automated flower classification over a large number of classes. In *2008 Sixth Indian conference on computer vision, graphics & image processing*, pages 722–729. IEEE.
- Nüsken, N. and Richter, L. (2021). Solving high-dimensional hamilton–jacobi–bellman pdes using neural networks: perspectives from the theory of controlled diffusions and measures on path space. *Partial differential equations and applications*, 2(4):48.
- Pidstrigach, J., Baker, E., Domingo-Enrich, C., Deligiannidis, G., and Nüsken, N. (2025). Conditioning diffusions using malliavin calculus. *arXiv preprint arXiv:2504.03461*.
- Richter, L., Boustati, A., Nüsken, N., Ruiz, F., and Akyildiz, O. D. (2020). Vargrad: a low-variance gradient estimator for variational inference. *Advances in Neural Information Processing Systems*, 33:13481–13492.

- Rombach, R., Blattmann, A., Lorenz, D., Esser, P., and Ommer, B. (2022). High-resolution image synthesis with latent diffusion models. In *Proceedings of the IEEE/CVF conference on computer vision and pattern recognition*, pages 10684–10695.
- Rout, L., Raoof, N., Daras, G., Caramanis, C., Dimakis, A., and Shakkottai, S. (2024). Solving linear inverse problems provably via posterior sampling with latent diffusion models. *Advances in Neural Information Processing Systems*, 36.
- Ruiz, N., Li, Y., Jampani, V., Pritch, Y., Rubinstein, M., and Aberman, K. (2023). Dreambooth: Fine tuning text-to-image diffusion models for subject-driven generation. In *Proceedings of the IEEE/CVF conference on computer vision and pattern recognition*, pages 22500–22510.
- Schulman, J., Wolski, F., Dhariwal, P., Radford, A., and Klimov, O. (2017). Proximal policy optimization algorithms. *arXiv preprint arXiv:1707.06347*.
- Sendera, M., Kim, M., Mittal, S., Lemos, P., Scimeca, L., Rector-Brooks, J., Adam, A., Bengio, Y., and Malkin, N. (2024). Improved off-policy training of diffusion samplers. In *The Thirty-eighth Annual Conference on Neural Information Processing Systems*.
- Shumailov, I., Shumaylov, Z., Zhao, Y., Gal, Y., Papernot, N., and Anderson, R. (2023). The curse of recursion: Training on generated data makes models forget. *arXiv preprint arXiv:2305.17493*.
- Song, B., Kwon, S. M., Zhang, Z., Hu, X., Qu, Q., and Shen, L. (2024). Solving inverse problems with latent diffusion models via hard data consistency. In *The Twelfth International Conference on Learning Representations*.
- Song, Y., Sohl-Dickstein, J., Kingma, D. P., Kumar, A., Ermon, S., and Poole, B. (2021). Score-based generative modeling through stochastic differential equations. In *ICLR*.
- Uehara, M., Zhao, Y., Wang, C., Li, X., Regev, A., Levine, S., and Biancalani, T. (2025). Reward-guided controlled generation for inference-time alignment in diffusion models: Tutorial and review. *arXiv preprint arXiv:2501.09685*.
- Vargas, F., Grathwohl, W. S., and Doucet, A. (2023a). Denoising diffusion samplers. In *The Eleventh International Conference on Learning Representations*.
- Vargas, F., Ovsianas, A., Fernandes, D., Girolami, M., Lawrence, N. D., and Nüsken, N. (2023b). Bayesian learning via neural schrödinger–föllmer flows. *Statistics and Computing*, 33(1):3.
- Vargas, F., Padhy, S., Blessing, D., and Nüsken, N. (2024). Transport meets variational inference: Controlled monte carlo diffusions. In *The Twelfth International Conference on Learning Representations*.
- Vargas, F., Thodoroff, P., Lamacraft, A., and Lawrence, N. (2021). Solving schrödinger bridges via maximum likelihood. *Entropy*, 23(9):1134.
- Venkatraman, S., Jain, M., Scimeca, L., Kim, M., Sendera, M., Hasan, M., Rowe, L., Mittal, S., Lemos, P., Bengio, E., Adam, A., Rector-Brooks, J., Bengio, Y., Berseth, G., and Malkin, N. (2024). Amortizing intractable inference in diffusion models for vision, language, and control. In *The Thirty-eighth Annual Conference on Neural Information Processing Systems*.
- Watson, J. L., Juergens, D., Bennett, N. R., Trippe, B. L., Yim, J., Eisenach, H. E., Ahern, W., Borst, A. J., Ragotte, R. J., Milles, L. F., et al. (2023). De novo design of protein structure and function with rfdiffusion. *Nature*, 620(7976):1089–1100.
- Xu, J., Liu, X., Wu, Y., Tong, Y., Li, Q., Ding, M., Tang, J., and Dong, Y. (2024). Imagereward: Learning and evaluating human preferences for text-to-image generation. *Advances in Neural Information Processing Systems*, 36.
- Zhang, L., Rao, A., and Agrawala, M. (2023). Adding conditional control to text-to-image diffusion models. In *Proceedings of the IEEE/CVF International Conference on Computer Vision*, pages 3836–3847.
- Zhang, Q. and Chen, Y. (2022). Path integral sampler: A stochastic control approach for sampling. In *International Conference on Learning Representations*.

Zhao, Y., Uehara, M., Scalia, G., Kung, S., Biancalani, T., Levine, S., and Hajiramezanali, E. (2025). Adding conditional control to diffusion models with reinforcement learning. In *The Thirteenth International Conference on Learning Representations*.

## A Radon-Nikodym derivative between SDEs.

To calculate the approximated importance weights, we make use of the RND between SDEs. In particular, we use the result from (Nüsken and Richter, 2021; Vargas et al., 2024).

**Proposition 6.** (RND between SDEs (Nüsken and Richter, 2021; Vargas et al., 2024)) Given the following SDEs

$$d\mathbf{Y}_t = a_t(\mathbf{Y}_t) dt + \sigma_t(\mathbf{Y}_t) d\overline{\mathbf{W}}_t, \quad \mathbf{Y}_0 \sim \mu, \quad (18)$$

$$d\mathbf{X}_t = b_t(\mathbf{X}_t) dt + \sigma_t(\mathbf{X}_t) d\overline{\mathbf{W}}_t, \quad \mathbf{X}_0 \sim \nu, \quad (19)$$

with path probabilities  $\overline{\mathbb{P}}_a$  and  $\overline{\mathbb{P}}_b$ , we get

$$\ln \left( \frac{d\overline{\mathbb{P}}_a}{d\overline{\mathbb{P}}_b} \right) (\mathbf{Z}) = \ln \left( \frac{d\mu}{d\nu} \right) (\mathbf{Z}_0) + \int_0^T \sigma_t^{-2} (a_t - b_t)(\mathbf{Z}_t) d\overline{\mathbf{Z}}_t + \frac{1}{2} \int_0^T \sigma_t^{-2} (b_t^2 - a_t^2)(\mathbf{Z}_t) dt, \quad (20)$$

and in particular, when evaluated on  $\mathbf{Y}$ :

$$\ln \left( \frac{d\overline{\mathbb{P}}_a}{d\overline{\mathbb{P}}_b} \right) (\mathbf{Y}) = \ln \left( \frac{d\mu}{d\nu} \right) (\mathbf{Y}_0) + \int_0^T \sigma_t^{-1} (a_t - b_t)(\mathbf{Y}_t) d\overline{\mathbf{W}}_t + \frac{1}{2} \int_0^T \sigma_t^{-2} \|b_t - a_t\|^2(\mathbf{Y}_t) dt. \quad (21)$$

Let  $\mathbb{P}_{\text{data}}$  be the path probability of

$$d\mathbf{X}_t = (f_t(\mathbf{X}_t) - \sigma_t^2 \nabla_{\mathbf{X}_t} \ln p_t(\mathbf{X}_t)) dt + \sigma_t d\overline{\mathbf{W}}_t, \quad \mathbf{X}_T \sim \mathcal{P}_T, \quad (22)$$

and  $\mathbb{P}_h$  the path probability of

$$d\mathbf{H}_t = (f_t(\mathbf{H}_t) - \sigma_t^2 (\nabla_{\mathbf{H}_t} \ln p_t(\mathbf{H}_t) + h_t(\mathbf{H}_t))) dt + \sigma_t d\overline{\mathbf{W}}_t, \quad \mathbf{H}_T \sim \mathcal{P}_T. \quad (23)$$

For the approximated importance weights we require the RND of  $\mathbb{P}_h$  with respect to  $\mathbb{P}_{\text{data}}$  evaluated at trajectories from  $\mathbb{P}_h$ . Let the drift of  $\mathbb{P}_{\text{data}}$  be given as  $a_t(\mathbf{x}) = f_t(\mathbf{x}) - \sigma_t^2 \nabla_{\mathbf{x}} \ln p_t(\mathbf{x})$  and the drift of  $\mathbb{P}_h$  as  $b_t(\mathbf{x}) = f_t(\mathbf{x}) - \sigma_t^2 \nabla_{\mathbf{x}} \ln p_t(\mathbf{x}) - \sigma_t^2 h_t(\mathbf{x})$ . In particular, we have  $a_t - b_t = \sigma_t^2 h_t$ . For readability, we do not omit the dependence on  $\mathbf{x}$  for the drift in the following. Using Proposition 6 we get,

$$\ln \left( \frac{d\mathbb{P}_{\text{data}}}{d\mathbb{P}_h} \right) (\mathbf{H}) = \int_0^T \sigma_t^{-2} (a_t - b_t) d\overline{\mathbf{H}}_t + \frac{1}{2} \int_0^T \sigma_t^{-2} (b_t^2 - a_t^2) dt \quad (24)$$

$$= \int_0^T \sigma_t^{-2} (a_t - b_t) b_t dt + \int_0^T \sigma_t^{-2} (a_t - b_t) \sigma_t d\overline{\mathbf{W}}_t + \frac{1}{2} \int_0^T \sigma_t^{-2} (b_t^2 - a_t^2) dt \quad (25)$$

$$= \frac{1}{2} \int_0^T \sigma_t^{-2} [2a_t b_t - 2b_t^2 + b_t^2 - a_t^2] dt + \int_0^T \sigma_t h_t d\overline{\mathbf{W}}_t \quad (26)$$

$$= -\frac{1}{2} \int_0^T \sigma_t^{-2} (b_t - a_t)^2 dt + \int_0^T \sigma_t h_t d\overline{\mathbf{W}}_t \quad (27)$$

$$= -\frac{1}{2} \int_0^T \sigma_t^2 \|h_t\|_2^2 dt + \int_0^T \sigma_t h_t d\overline{\mathbf{W}}_t, \quad (28)$$

evaluated on a trajectory  $\mathbf{H}$  from  $\mathbb{P}_h$ .

### A.1 Discrete Version for DDPM

We can also express the RND in the discrete setting. For this derivation, we make use of the DDPM schedule (Ho et al., 2020). The generalisation to different schedules is straightforward. The path probability of the pre-trained model is given as

$$p_\theta^{\text{data}}(\mathbf{x}_0, \dots, \mathbf{x}_T) = p_T(\mathbf{x}_T) \prod_{t=1}^T p_\theta^{\text{data}}(\mathbf{x}_{t-1} | \mathbf{x}_t), \quad p_\theta^{\text{data}}(\mathbf{x}_{t-1} | \mathbf{x}_t) = \mathcal{N}(\mathbf{x}_{t-1} | \mu_\theta(\mathbf{x}_t, t); \tilde{\beta}_t^2 I) \quad (29)$$

where the mean is parametrised as  $\mu_\theta(\mathbf{x}_t, t) = \frac{1}{\sqrt{\alpha_t}}(\mathbf{x}_t - \frac{1-\alpha_t}{\sqrt{1-\alpha_t}}\epsilon_\theta(\mathbf{x}_t, t))$ . Similar, we have path probabilities for the fine-tuned model as

$$p_\varphi^h(\mathbf{x}_0, \dots, \mathbf{x}_T) = p_T(\mathbf{x}_T) \prod_{t=1}^T p_\varphi^h(\mathbf{x}_{t-1}|\mathbf{x}_t), \quad p_\varphi^h(\mathbf{x}_{t-1}|\mathbf{x}_t) = \mathcal{N}(\mathbf{x}_{t-1}|\mu_h(\mathbf{x}_t, t); \tilde{\beta}_t^2 I), \quad (30)$$

with mean  $\mu_h(\mathbf{x}_t, t) = \mu_\theta(\mathbf{x}_t, t) + \Delta_h(\mathbf{x}_t, t)$  is the original mean plus a delta given by the  $h$ -transform. We use  $\tilde{\beta}_t = \sqrt{\frac{1-\tilde{\alpha}_t-1}{1-\tilde{\alpha}_t}}\beta_t$  for the standard deviation of the reverse kernel. Using this setting, we can write the RND as

$$\ln \left( \frac{p_\theta^{\text{data}}(\mathbf{x}_0, \dots, \mathbf{x}_T)}{p_\varphi^h(\mathbf{x}_0, \dots, \mathbf{x}_T)} \right) = \sum_{t=1}^T \ln \left( \frac{p_\theta^{\text{data}}(\mathbf{x}_{t-1}|\mathbf{x}_t)}{p_\varphi^h(\mathbf{x}_{t-1}|\mathbf{x}_t)} \right), \quad (31)$$

where we assumed that the terminal distribution  $p_T$  is the same for both diffusion models. The log ratio of two Gaussian reduces to

$$\ln \left( \frac{\mathcal{N}(x; \mu_1, \Sigma_1)}{\mathcal{N}(x; \mu_2, \Sigma_2)} \right) = -\frac{1}{2}[(x - \mu_1)^T \Sigma_1^{-1} (x - \mu_1) - (x - \mu_2)^T \Sigma_2^{-1} (x - \mu_2)] + \frac{1}{2} \ln \frac{|\Sigma_2|}{|\Sigma_1|}, \quad (32)$$

which gets us

$$\ln \left( \frac{p_\theta^{\text{data}}(\mathbf{x}_{t-1}|\mathbf{x}_t)}{p_\varphi^h(\mathbf{x}_{t-1}|\mathbf{x}_t)} \right) = -\frac{1}{2\tilde{\beta}_t^2} [\|\mathbf{x}_{t-1} - \mu_\theta(\mathbf{x}_t, t)\|_2^2 - \|\mathbf{x}_{t-1} - \mu_h(\mathbf{x}_t, t)\|_2^2]. \quad (33)$$

To further simplify these terms, we need some information about the trajectory  $\mathbf{x}_0, \dots, \mathbf{x}_T$ . In particular, we assume that we have a *trajectory sampled from the fine-tuned model*, i.e.,

$$\mathbf{x}_{t-1} = \mu_h(\mathbf{x}_t, t) + \tilde{\beta}_t \epsilon, \quad \epsilon \sim \mathcal{N}(0, I). \quad (34)$$

Given the parametrisation of the mean in the diffusion model

$$\mu_\theta(\mathbf{x}_t, t) = \frac{1}{\sqrt{\alpha_t}} \left( \mathbf{x}_t - \frac{1-\alpha_t}{\sqrt{1-\alpha_t}} \epsilon_\theta(\mathbf{x}_t, t) \right), \quad (35)$$

$$\mu_h(\mathbf{x}_t, t) = \frac{1}{\sqrt{\alpha_t}} \left( \mathbf{x}_t - \frac{1-\alpha_t}{\sqrt{1-\alpha_t}} \epsilon_\theta(\mathbf{x}_t, t) - \frac{1-\alpha_t}{\sqrt{1-\tilde{\alpha}_t}} h_\varphi(\mathbf{x}_t, t) \right), \quad (36)$$

we can reduce the terms on the RHS of Equation (33) to

$$\|\mathbf{x}_{t-1} - \mu_\theta(\mathbf{x}_t, t)\|_2^2 - \|\mathbf{x}_{t-1} - \mu_h(\mathbf{x}_t, t)\|_2^2 \quad (37)$$

$$= \|\mu_h(\mathbf{x}_t, t) + \tilde{\beta}_t \epsilon - \mu_\theta(\mathbf{x}_t, t)\|_2^2 - \|\mu_h(\mathbf{x}_t, t) + \tilde{\beta}_t \epsilon - \mu_h(\mathbf{x}_t, t)\|_2^2 \quad (38)$$

$$= \|\Delta_h(\mathbf{x}_t, t) + \tilde{\beta}_t \epsilon\|_2^2 - \|\tilde{\beta}_t \epsilon\|_2^2. \quad (39)$$

Combining Equation (39) and Equation (33), we obtain

$$\ln \left( \frac{p_\theta^{\text{data}}(\mathbf{x}_{t-1}|\mathbf{x}_t)}{p_\varphi^h(\mathbf{x}_{t-1}|\mathbf{x}_t)} \right) = -\frac{1}{2\tilde{\beta}_t^2} [\|\mathbf{x}_{t-1} - \mu_\theta(\mathbf{x}_t, t)\|_2^2 - \|\mathbf{x}_{t-1} - \mu_h(\mathbf{x}_t, t)\|_2^2] \quad (40)$$

$$= -\frac{1}{2\tilde{\beta}_t^2} [\|\Delta_h(\mathbf{x}_t, t) + \tilde{\beta}_t \epsilon\|_2^2 - \|\tilde{\beta}_t \epsilon\|_2^2] \quad (41)$$

$$= -\frac{1}{2\tilde{\beta}_t^2} [\|\Delta_h(\mathbf{x}_t, t)\|_2^2 + 2\Delta_h(\mathbf{x}_t, t)^\top \tilde{\beta}_t \epsilon + \|\tilde{\beta}_t \epsilon\|_2^2 - \|\tilde{\beta}_t \epsilon\|_2^2] \quad (42)$$

$$= -\frac{1}{2\tilde{\beta}_t^2} \|\Delta_h(\mathbf{x}_t, t)\|_2^2 - \frac{1}{\tilde{\beta}_t} \Delta_h(\mathbf{x}_t, t)^\top \epsilon. \quad (43)$$

For the full RND we obtain

$$\sum_{t=1}^T \ln \left( \frac{p_\theta^{\text{data}}(\mathbf{x}_{t-1}|\mathbf{x}_t)}{p_\varphi^h(\mathbf{x}_{t-1}|\mathbf{x}_t)} \right) = \sum_{t=1}^T \left[ -\frac{1}{2}\tilde{\beta}_t^{-2} \|\Delta_h(\mathbf{x}_t, t)\|_2^2 + \tilde{\beta}_t^{-1} \Delta_h(\mathbf{x}_t, t)^\top \epsilon \right], \quad (44)$$

which mimics a discretised version of the continuous RND in Equation (28).

## B Resampling Step

### B.1 Proof to Theorem 5

*Proof.* Part (i) is a Bayes theorem.

The proof of part (ii) follows similar ideas as (Hertrich and Gruhlke, 2024, Prop 8 (ii)). To this end, let  $Z = \mathbb{E}_{\mathbf{x}_{[0,T]} \sim \mathbb{P}_h} [\alpha(\mathbf{x}_{[0,T]})]$ . Then, we can estimate by Jensens' inequality that

$$\begin{aligned} -\ln(Z) &= -\ln \left( \mathbb{E}_{\mathbf{x}_{[0,T]} \sim \mathbb{P}_h} \left[ \min \left( \frac{d\mathbb{P}_{\text{data}}}{d\mathbb{P}_h}(\mathbf{x}_{[0,T]}) \frac{\exp(r(\mathbf{x}_0))}{c}, 1 \right) \right] \right) \\ &\leq -\mathbb{E}_{\mathbf{x}_{[0,T]} \sim \mathbb{P}_h} \left[ \ln \left( \min \left( \frac{d\mathbb{P}_{\text{data}}}{d\mathbb{P}_h}(\mathbf{x}_{[0,T]}) \frac{\exp(r(\mathbf{x}_0))}{c}, 1 \right) \right) \right] \\ &= -\mathbb{E}_{\mathbf{x}_{[0,T]} \sim \mathbb{P}_h} \left[ \min \left( \ln \left( \frac{d\mathbb{P}_{\text{data}}}{d\mathbb{P}_h}(\mathbf{x}_{[0,T]}) \frac{\exp(r(\mathbf{x}_0))}{c} \right), 0 \right) \right] \\ &= \mathbb{E}_{\mathbf{x}_{[0,T]} \sim \mathbb{P}_h} \left[ \max \left( \ln \left( \frac{d\mathbb{P}_h}{d\mathbb{P}_{\text{data}}}(\mathbf{x}_{[0,T]}) \frac{c}{\exp(r(\mathbf{x}_0))} \right), 0 \right) \right] \end{aligned}$$

On the other side, we have by definition that

$$\begin{aligned} \text{KL}(\tilde{\mathbb{P}}_h, \mathbb{P}_{\text{data}}) - \mathbb{E}_{\mathbf{x}_{[0,T]} \sim \tilde{\mathbb{P}}_h} [r(\mathbf{x}_0)] &= \mathbb{E}_{\mathbf{x}_{[0,T]} \sim \tilde{\mathbb{P}}_h} \left[ \ln \left( \frac{d\tilde{\mathbb{P}}_h}{d\mathbb{P}_{\text{data}}}(\mathbf{x}_{[0,T]}) \right) \right] - \mathbb{E}_{\mathbf{x}_{[0,T]} \sim \tilde{\mathbb{P}}_h} [r(\mathbf{x}_0)] \\ &= \mathbb{E}_{\mathbf{x}_{[0,T]} \sim \tilde{\mathbb{P}}_h} \left[ \ln \left( \frac{cZ}{\exp(r(\mathbf{x}_0))} \frac{d\tilde{\mathbb{P}}_h}{d\mathbb{P}_{\text{data}}}(\mathbf{x}_{[0,T]}) \right) \right] - \ln(cZ). \end{aligned}$$

By taking the expectation over  $\mathbb{P}_h$  instead of  $\tilde{\mathbb{P}}_h$  this is equal to

$$\mathbb{E}_{\mathbf{x}_{[0,T]} \sim \mathbb{P}_h} \left[ \frac{d\tilde{\mathbb{P}}_h}{d\mathbb{P}_h}(\mathbf{x}_{[0,T]}) \ln \left( \frac{cZ}{\exp(r(\mathbf{x}_0))} \frac{d\tilde{\mathbb{P}}_h}{d\mathbb{P}_h}(\mathbf{x}_{[0,T]}) \frac{d\mathbb{P}_h}{d\mathbb{P}_{\text{data}}}(\mathbf{x}_{[0,T]}) \right) \right] - \ln(cZ).$$

Inserting the formula from part (i) and then the definition of  $\alpha$ , this is equal to

$$\begin{aligned} &\mathbb{E}_{\mathbf{x}_{[0,T]} \sim \mathbb{P}_h} \left[ \frac{\alpha(\mathbf{x}_{[0,T]})}{Z} \ln \left( \frac{c}{\exp(r(\mathbf{x}))} \alpha(\mathbf{x}_{[0,T]}) \frac{d\mathbb{P}_h}{d\mathbb{P}_{\text{data}}}(\mathbf{x}_{[0,T]}) \right) \right] - \ln(cZ) \\ &= \mathbb{E}_{\mathbf{x}_{[0,T]} \sim \mathbb{P}_h} \left[ \frac{\alpha(\mathbf{x}_{[0,T]})}{Z} \ln \left( \frac{c}{\exp(r(\mathbf{x}))} \min \left( 1, \frac{d\mathbb{P}_{\text{data}}}{d\mathbb{P}_h}(\mathbf{x}_{[0,T]}) \frac{\exp(r(\mathbf{x}_0))}{c} \right) \frac{d\mathbb{P}_h}{d\mathbb{P}_{\text{data}}}(\mathbf{x}_{[0,T]}) \right) \right] - \ln(cZ) \\ &= \mathbb{E}_{\mathbf{x}_{[0,T]} \sim \mathbb{P}_h} \left[ \frac{\alpha(\mathbf{x}_{[0,T]})}{Z} \ln \left( \min \left( \frac{d\mathbb{P}_h}{d\mathbb{P}_{\text{data}}}(\mathbf{x}_{[0,T]}) \frac{c}{\exp(r(\mathbf{x}_0))}, 1 \right) \right) \right] - \ln(cZ) \\ &= \mathbb{E}_{\mathbf{x}_{[0,T]} \sim \mathbb{P}_h} \left[ \frac{\alpha(\mathbf{x}_{[0,T]})}{Z} \min \left( \ln \left( \frac{d\mathbb{P}_h}{d\mathbb{P}_{\text{data}}}(\mathbf{x}_{[0,T]}) \frac{c}{\exp(r(\mathbf{x}_0))} \right), 0 \right) \right] - \ln(cZ) \\ &= \frac{1}{Z} \mathbb{E}_{\mathbf{x}_{[0,T]} \sim \mathbb{P}_h} \left[ \min \left( \alpha(\mathbf{x}_{[0,T]}) \ln \left( \frac{d\mathbb{P}_h}{d\mathbb{P}_{\text{data}}}(\mathbf{x}_{[0,T]}) \frac{c}{\exp(r(\mathbf{x}_0))} \right), 0 \right) \right] - \ln(cZ) \\ &= \frac{1}{Z} \mathbb{E}_{\mathbf{x}_{[0,T]} \sim \mathbb{P}_h} \left[ \min \left( \min \left( 1, \frac{d\mathbb{P}_{\text{data}}}{d\mathbb{P}_h}(\mathbf{x}_{[0,T]}) \frac{\exp(r(\mathbf{x}_0))}{c} \right) \ln \left( \frac{d\mathbb{P}_h}{d\mathbb{P}_{\text{data}}}(\mathbf{x}_{[0,T]}) \frac{c}{\exp(r(\mathbf{x}_0))} \right), 0 \right) \right] - \ln(cZ). \end{aligned}$$

Since  $1 \leq \frac{d\mathbb{P}_{\text{data}}}{d\mathbb{P}_h}(\mathbf{x}_{[0,T]}) \frac{\exp(r(\mathbf{x}_0))}{c}$  if and only if  $\ln \left( \frac{d\mathbb{P}_h}{d\mathbb{P}_{\text{data}}}(\mathbf{x}_{[0,T]}) \frac{c}{\exp(r(\mathbf{x}_0))} \right) \leq 0$  the minimum is attained either for both min in the above formula in the first argument or it is attained for both min in the second argument. Consequently the above formula is equal to

$$\begin{aligned} &\frac{1}{Z} \mathbb{E}_{\mathbf{x}_{[0,T]} \sim \mathbb{P}_h} \left[ \min \left( \ln \left( \frac{d\mathbb{P}_h}{d\mathbb{P}_{\text{data}}}(\mathbf{x}_{[0,T]}) \frac{c}{\exp(r(\mathbf{x}_0))} \right), 0 \right) \right] - \ln(cZ) \\ &\leq \mathbb{E}_{\mathbf{x}_{[0,T]} \sim \mathbb{P}_h} \left[ \min \left( \ln \left( \frac{d\mathbb{P}_h}{d\mathbb{P}_{\text{data}}}(\mathbf{x}_{[0,T]}) \frac{c}{\exp(r(\mathbf{x}_0))} \right), 0 \right) \right] - \ln(Z) - \ln(c), \end{aligned}$$



where the inequality comes from the fact that  $Z \in (0, 1]$  and that the expectation is non-positive (since the integrand is non-positive). Inserting the formula of  $-\ln(Z)$  from the beginning of the proof, this is equal to

$$\begin{aligned}
& \mathbb{E}_{\mathbf{x}_{[0:T]} \sim \mathbb{P}_h} \left[ \min \left( \ln \left( \frac{d\mathbb{P}_h}{d\mathbb{P}_{\text{data}}}(\mathbf{x}_{[0:T]}) \frac{c}{\exp(r(\mathbf{x}_0))} \right), 0 \right) \right] \\
& + \mathbb{E}_{\mathbf{x}_{[0:T]} \sim \mathbb{P}_h} \left[ \max \left( \ln \left( \frac{d\mathbb{P}_h}{d\mathbb{P}_{\text{data}}}(\mathbf{x}_{[0:T]}) \frac{c}{\exp(r(\mathbf{x}_0))} \right), 0 \right) \right] - \ln(c) \\
& = \mathbb{E}_{\mathbf{x}_{[0:T]} \sim \mathbb{P}_h} \left[ \ln \left( \frac{d\mathbb{P}_h}{d\mathbb{P}_{\text{data}}}(\mathbf{x}_{[0:T]}) \frac{c}{\exp(r(\mathbf{x}_0))} \right) \right] - \ln(c) \\
& = \mathbb{E}_{\mathbf{x}_{[0:T]} \sim \mathbb{P}_h} \left[ \ln \left( \frac{d\mathbb{P}_h}{d\mathbb{P}_{\text{data}}}(\mathbf{x}_{[0:T]}) \right) \right] - \mathbb{E}_{\mathbf{x}_{[0:T]} \sim \mathbb{P}_h} [r(\mathbf{x}_0)] \\
& = \text{KL}(\mathbb{P}_h, \mathbb{P}_{\text{data}}) - \mathbb{E}_{\mathbf{x}_{[0:T]} \sim \mathbb{P}_h} [r(\mathbf{x}_0)].
\end{aligned}$$

This concludes the proof of part (ii).

For part (iii), we observe that the loss in (15) is learning the marginal score of a forward SDE (in our case a VP-SDE intiliased at  $\tilde{\mathbb{P}}_h^0$ , by construction the associated path measure of this process is given by (See appendix A (Vargas et al., 2023a) for a similar sketch) <sup>2</sup>:

$$\mathbb{P}_{h^*}(\cdot) = \mathbb{P}_{\text{forward}}(\cdot | \mathbf{x}_0) \tilde{\mathbb{P}}_h^0(\mathbf{x}_0) \quad (45)$$

$$= \mathbb{P}_{\text{forward}}(\cdot | \mathbf{x}_0) \mathbb{P}_{\text{data}}(\mathbf{x}_0) \cdot \frac{\tilde{\mathbb{P}}_h^0}{p_{\text{data}}}(\mathbf{x}_0) \quad (46)$$

$$= \frac{\tilde{\mathbb{P}}_h^0}{p_{\text{data}}} \mathbb{P}_{\text{data}}(\cdot) \quad (47)$$

Thus, the path measure minimising the score-matching loss satisfies

$$\mathbb{P}_{h^*} = \frac{\tilde{\mathbb{P}}_h^0}{p_{\text{data}}} \mathbb{P}_{\text{data}} \quad (48)$$

Then it follows that

$$\text{KL}(\mathbb{P}_{h^*} || \mathbb{P}_{\text{data}}) = \mathbb{E}_{\mathbf{x}_{[0:T]} \sim \mathbb{P}_{h^*}} \left[ \ln \left( \frac{d\mathbb{P}_{\text{data}}}{d\mathbb{P}_{h^*}}(\mathbf{x}_{[0:T]}) \frac{\tilde{\mathbb{P}}_h^0(\mathbf{x}_0)}{p_{\text{data}}(\mathbf{x}_0)} \right) \right] \quad (49)$$

$$= \mathbb{E}_{\mathbf{x}_{[0:T]} \sim \frac{\tilde{\mathbb{P}}_h^0}{p_{\text{data}}} \mathbb{P}_{\text{data}}} \left[ \ln \left( \frac{\tilde{\mathbb{P}}_h^0(\mathbf{x}_0)}{p_{\text{data}}(\mathbf{x}_0)} \right) \right] \quad (50)$$

$$= \mathbb{E}_{\mathbf{x}_0 \sim \tilde{\mathbb{P}}_h^0} \left[ \ln \left( \frac{\tilde{\mathbb{P}}_h^0(\mathbf{x}_0)}{p_{\text{data}}(\mathbf{x}_0)} \right) \right] = \text{KL}(\tilde{\mathbb{P}}_h^0, p_{\text{data}}) \quad (51)$$

Via the disintegration theorem (Léonard, 2014, Theorem 1.6. and Theorem 2.4), the KL divergence can be decomposed as

$$\text{KL}(\tilde{\mathbb{P}}_h, \mathbb{P}_{\text{data}}) = \mathbb{E}[\text{KL}(\tilde{\mathbb{P}}_h(\cdot | \mathbf{x}_0), \mathbb{P}_{\text{data}}(\cdot | \mathbf{x}_0))] + \text{KL}(\tilde{\mathbb{P}}_h^0, p_{\text{data}}) \quad (52)$$

Where  $\mathbb{E}[\text{KL}(\tilde{\mathbb{P}}_h(\cdot | \mathbf{x}_0), \mathbb{P}_{\text{data}}(\cdot | \mathbf{x}_0))] \geq 0$  and thus

$$\text{KL}(\mathbb{P}_{h^*}, \mathbb{P}_{\text{data}}) = \text{KL}(\tilde{\mathbb{P}}_h^0, p_{\text{data}}) \leq \text{KL}(\tilde{\mathbb{P}}_h, \mathbb{P}_{\text{data}}).$$

Since the marginals of  $\mathbb{P}_{h^*}$  and  $\tilde{\mathbb{P}}_h$  at time 0 coincide, we obtain

$$\mathcal{F}(\mathbb{P}_{h^*}) = \text{KL}(\mathbb{P}_{h^*}, \mathbb{P}_{\text{data}}) - \mathbb{E}_{\mathbf{x}_{[0:T]} \sim \mathbb{P}_{h^*}} [r(\mathbf{x}_0)] \quad (53)$$

$$= \text{KL}(\mathbb{P}_{h^*}, \mathbb{P}_{\text{data}}) - \mathbb{E}_{\mathbf{x}_{[0:T]} \sim \tilde{\mathbb{P}}_h} [r(\mathbf{x}_0)] \quad (54)$$

$$\leq \text{KL}(\tilde{\mathbb{P}}_h, \mathbb{P}_{\text{data}}) - \mathbb{E}_{\mathbf{x}_{[0:T]} \sim \tilde{\mathbb{P}}_h} [r(\mathbf{x}_0)] = \mathcal{F}(\tilde{\mathbb{P}}_h), \quad (55)$$

which shows the first inequality from the claim. The second inequality was proven in part (ii).  $\square$

<sup>2</sup>Note we slightly abuse notation here as these equalities are meant to be understood in an RND sense but we omit the full ratio notation for brevity.

## C Experimental Details and Additional Results

### C.1 2D Toy Example

We train the initial diffusion model on a Gaussian mixture model with modes 25 equally weighted modes where the set of means is defined by  $\{-2.5, -1.25, 0, 1.25, 2.5\}^2$  and the covariance matrix is given by  $0.1I$ . The reward function  $r$  is defined as the negative log likelihood function of a GMM with four modes with means  $(-2.5, 1.25)$ ,  $(-1.25, 2.5)$ ,  $(1.25, 0)$  and  $(2.5, -1.25)$ , covariance matrix  $0.1I$  and mode weights  $\frac{1}{8}$ ,  $\frac{1}{8}$ ,  $\frac{5}{8}$  and  $\frac{1}{8}$ . For classifier guidance, we choose the parameter  $\gamma$  by maximising the expected reward, which is  $\gamma = 0.3$ . For the importance and reward-only fine-tuning we use a batch size of 4096, a buffer size of 6000 and a KL regularisation with  $\alpha_{\text{KL}} = 0.06$ . We initialise the buffer with samples from the initial score-model. Then we perform 20 fine-tuning steps with 500 gradient updates per iteration. We choose  $c$  such that 40% of the samples will be rejected. The total training time is approximately 1min on a single NVIDIA GeForce RTX 4090.

### C.2 Posterior Sampling for inverse problems

We train a unconditional score-based diffusion model on the Flowers dataset with the VP-SDE with  $\beta_{\min} = 0.1$  and  $\beta_{\max} = 20.0$ . We parametrise the score model using a small Attention UNet (Dhariwal and Nichol, 2021) with approx. 10M parameters. We parametrise the  $h$ -transform as in Equation (16) with approx. 0.8M parameters. The scaling network  $\text{NN}_2(t)$  was initialised as a linear function going from 0 to 0.001. In this already at the start of training, we obtain trajectories which are similar to the ground truth leading to more stable optimisation. We used 50 importance fine-tuning iterations with 20 gradient updates per iteration. For every iteration we sampled 64 new trajectories and used a resampling rate of 50%. We used a maximal buffer size of 256 images and no KL-regularisation. The total training time is approximately 8min on a single NVIDIA GeForce RTX 4090.

At the start of fine-tuning the end points  $\mathbf{x}_0$  of most trajectories are not consistent with the measurements  $\mathbf{y}^\delta$ , leading to a low reward  $r(\mathbf{x}_0; \mathbf{y}^\delta)$ . This can sometimes lead to instabilities at the start of training, if no valid high reward trajectory was sampled. We found that it was helpful to amortise over measurements, such that we consider the amortised loss function

$$\mathcal{L}_{FT}(g) = \mathbb{E}_{\substack{\mathbf{x}_0 \sim \tilde{\mathbb{P}}_{h,k}^0, \mathbf{y} \sim p^{\text{hkd}}(\mathbf{y}|\mathbf{x}_0) \\ t \sim \text{U}(0,T), \mathbf{x}_t \sim \tilde{p}_{t|0}(\cdot|\mathbf{x}_0)}} \left[ \left\| (g_t(\mathbf{x}_t, \mathbf{y}) + s_t(\mathbf{x}_t)) - \nabla_{\mathbf{x}_t} \ln \tilde{p}_{t|0}(\mathbf{x}_t|\mathbf{x}_0) \right\|^2 \right], \quad (56)$$

where the simulated measurements  $\mathbf{y} \sim p^{\text{hkd}}(\mathbf{y}|\mathbf{x}_0)$  are added as an additional input to the  $h$ -transform.

### C.3 Class conditional sampling

We pre-train a score-based diffusion model on the MNIST dataset with the VP-SDE with  $\beta_{\min} = 0.1$  and  $\beta_{\max} = 20.0$ . We parametrise the score model using a small Attention UNet (Dhariwal and Nichol, 2021) with approx. 1.1M parameters. We parametrise the  $h$ -transform as in Equation (16) with approx. 0.8M parameters. For all experiments, we use a batch size of 256, a buffer size of 2048 and a reward scaling  $\lambda = 4.0$ . We perform 50 importance fine-tuning iterations with 50 gradient updates per iterations. We use the KL regulariser with  $\alpha_{\text{KL}} = 0.001$ . Lastly, we adaptively choose  $c$  such that 10% of the samples will be accepted for the first 10 steps. After the initial 10 steps, we accept 30% of the samples. We start with 10% as MNIST has 10 classes with roughly similar class probabilities. The total training time is about 10min on a single NVIDIA GeForce RTX 4090.

For the comparison methods in Table 1, we use classifier guidance and online fine-tuning. For classifier guidance, we used a scaling  $\gamma = 4.5$  maximising sample quality. For online fine-tuning we directly minimise (10) using VarGrad (Richter et al., 2020). VarGrad enables us to detach the trajectory from the backpropagation, thus saving memory cost and enabling us to train with a larger batch size. In particular, we use the formulation in Denker et al. (2024) as

$$D_{\log\text{var}}(\mathbb{P}_h, \mathbb{P}_{\text{data}}; \mathbb{W}) = \text{Var}_{\mathbf{H}_{0:T}^{g_t} \sim \mathbb{W}} \left[ \ln \frac{d\mathbb{P}_h}{d\mathbb{P}_{\text{data}}}(\mathbf{H}_{0:T}^{g_t}) \right], \quad (57)$$

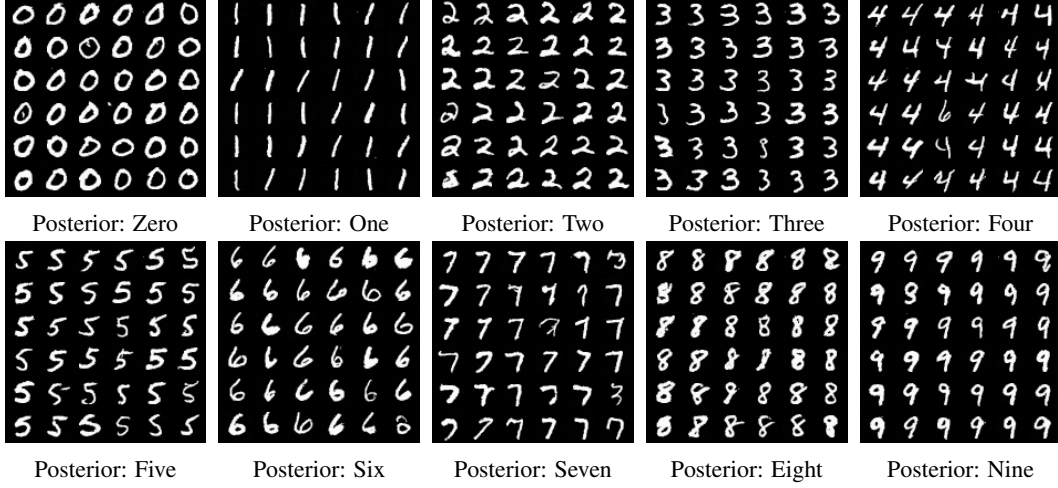


Figure 5: Class conditional sampling for MNIST for all classes. We used the same initial seed. The model for "Posterior: Four" has apparently not fully converged, as we still see a "6" in the image.

evaluated at a reference process  $\mathbb{W} = \text{Law}(\mathbf{H}_{0:T}^{g_t})$ , given by

$$\begin{aligned} \mathbf{H}_T &\sim Q_T^{f_t}[p_{\text{tilted}}] \\ d\mathbf{H}_t &= (f_t(\mathbf{H}_t) - \sigma_t^2(s_t(\mathbf{H}_t) + g_t(\mathbf{H}_t))) dt + \sigma_t d\overline{\mathbf{W}}_t. \end{aligned} \quad (58)$$

In particular, if we choose  $g_t = \text{stop\_grad}(h_t)$  as a detached copy of the current estimation  $h_t$ , we obtain

$$\begin{aligned} \ln \frac{d\mathbb{P}_h}{d\mathbb{P}_{\text{data}}}(\mathbf{H}_{0:T}^{g_t}) &= -\frac{1}{2} \int_0^T \sigma_t^2 \|h_t(\mathbf{H}_t^{g_t})\|^2 dt + \int_0^T \sigma_t^2 (g_t^\top h_t)(\mathbf{H}_t^{g_t}) dt - r(\mathbf{x}_0^{g_t}) \\ &\quad + \int_0^T \sigma_t h_t^\top(\mathbf{H}_t^{g_t}) d\overline{\mathbf{W}}_t, \end{aligned} \quad (59)$$

using the RND for time reverse SDEs see Equation 64 in (Vargas et al., 2024). We use the same reward-informed network architecture to parametrise  $h_t$ .

In Figure 5 we show the posterior for all 10 classes. For all experiments, we chose the same hyperparameters as well as the same initial seed for the samples presented. We observe that these settings work for most classes. However, for class "Four" we see a single digit "Six" in the image, giving evidence that this particular model has not fully converged.

#### C.4 Reward Fine-tuning

Diffusion models can be used for conditional generation via classifier free guidance (Ho and Salimans, 2022). In classifier free guidance both an unconditional  $\epsilon_t^\theta(\mathbf{x}_t)$  and a conditional  $\epsilon_t^\theta(\mathbf{x}_t, c)$  noise-prediction model are learned by randomly masking out the text prompt  $c$ . During sampling the linear combination  $\bar{\epsilon}_t^\theta(\mathbf{x}_t, t) = (1 + w)\epsilon_t^\theta(\mathbf{x}_t, c) - w\epsilon_t^\theta(\mathbf{x}_t)$ , with a guidance scale  $w$ , is used. Despite the progress in training text-to-image diffusion models, the samples are not always aligned with human preferences. For the alignment we make use of ImageReward-v1.0, a human preference reward model (Xu et al., 2024). These reward models  $r(\mathbf{x}; c)$  are trained to produce a reward from a given text prompt  $c$  and an image  $\mathbf{x}$ , corresponding to human preferences. Here, we learn the tilted distribution for a given text prompt and directly fine-tune the classifier free model  $\bar{\epsilon}_t^\theta(\mathbf{x}_t, t)$  using the LoRA parametrisation (Hu et al., 2022) instead of the reward-informed parametrisation. We use a LoRA for all attention layers with a rank of 10. We used a buffer of 64 images and sample 128 new images at every iteration, the parameter  $c$  was chosen such that 10% of the images were accepted. We used a total of 25 iterations, where we did 40 gradient descent steps with an effective batch size of 64 at each iteration (batch of 4 and 16 gradient accumulation steps). Fine-tuning took about 7 hours on a single NVIDIA GeForce RTX 4090. We used the AdamW optimiser (Loshchilov and Hutter, 2019) with a learning rate of  $1 \times 10^{-4}$  and a cosine decay to  $1 \times 10^{-5}$ . For the final

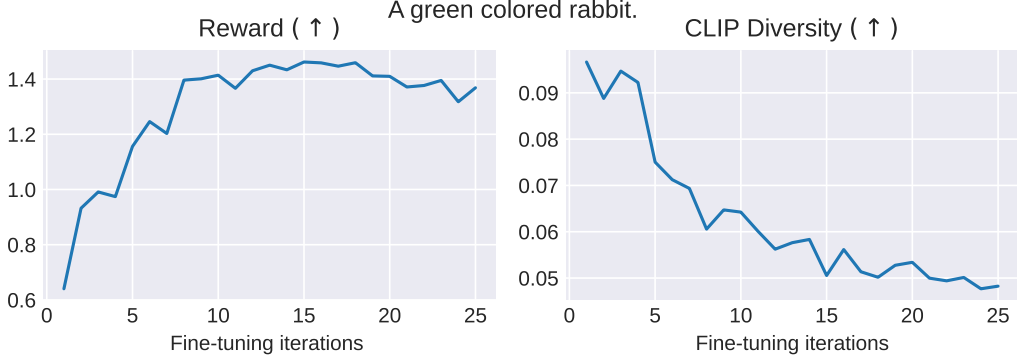


Figure 6: Reward and diversity for text-to-image fine-tuning on "A green colored rabbit." during training. As known for LoRA fine-tuning the diversity decreases over iterations.



Figure 7: Samples for the base model, DPOK, Adjoint Matching and our importance FT for the prompt "Two roses in a vase.". Images were generated using the same seed.

sampling evaluation we used the DDIM scheduler with 50 time steps. We used a guidance scale of 5.0 for Stable Diffusion.

We compare against Top-K sampling, DPOK (Fan et al., 2024) and Adjoint Matching (Domingo-Enrich et al., 2025). We give the experimental details in the following paragraphs.

Additional images are shown in Figure 7 and Figure 8. We also observe the reward and diversity during iterations, see Figure 6.

**Top-K Sampling** is a widely known approach to increase the performance of text-to-image diffusion models without additional training. Here, we sample a batch of  $K$  images and only return the image with the highest reward. In our implementation we use  $K = 6$ . Top-K sampling is easy to implement and requires no additional training loss, but often decrease diversity and increased the sampling time by a factor of  $K$ .

**DPOK** was proposed by (Fan et al., 2024) to fine-tune diffusion models using a differentiable reward. We use the implementation by the authors using the provided hyperparameters<sup>3</sup>. DPOK used LoRA for the fine-tuning parametrisation, we use the default parameters as suggested by the authors. Fine-tuning takes 28h on a single A100.

**Adjoint Matching** reformulates fine-tuning as a stochastic optimal control problem and casting it as a regression problem. We use the implementation by the authors with the provided hyperparameters<sup>4</sup>. Adjoint Matching fine-tunes the full model and does not use LoRA. This requires large GPUs and the experiments cannot be performed on a NVIDIA Geforce RTX 4090. We use the adjoint matching variant which uses CFG to sample trajectories, but not in the adjoint computation. This setting is not covered by theory, but leads to the best empirical results.

<sup>3</sup><https://github.com/google-research/google-research/tree/master/dpok>

<sup>4</sup><https://github.com/microsoft/soc-fine-tuning-sd>



Figure 8: Samples for the base model, DPOK, Adjoint Matching and our importance FT for the prompt "Two dogs in the park.". Images were generated using the same seed.